DOI 10.5162/IMCS2012/4.3.5

One-pot Hydrothermal Synthesis of SnO and SnO_2 Nanostructures: Enhanced H_2 Sensing Attributed to in-situ p-n Junctions

*Arunkumar.S, Pratyay Basak, L. Satyanarayana, Sunkara V. Manorama**
Nanomaterials Laboratory, Inorganic and Physical Chemistry Division,
CSIR-Indian Institute of Chemical Technology, Uppal Road,
Hyderabad-500007, Andhra Pradesh, India.
manorama@iict.res.in

Abstract:
Herein, we present a novel hydrothermal synthetic approach for the formation of SnO/SnO_2 nanorods and their assembly into micro cubes as an effective gas sensing material. The synthesized materials were characterized by powder x-ray diffraction, Micro-Raman, FT-IR, XPS, and thermogravimetry. Morphological evaluations by SEM revealed the rods of about 10 nm and cube about 6 um. Electrical characterization results attribute the enhanced hydrogen gas sensing response to the formation of SnO_2/SnO local p-n junctions. Significantly improved sensor response and sensitivity could be achieved using Pd functionalization. Further, the anomalous room temperature ferromagnetic behavior of the as synthesized materials and its consequence on the enhanced sensing property is discussed.

Key words: SnO_2/SnO, p-n junction, Hydrogen sensor, Room temperature sensing.

1. Introduction

Hydrogen is the next generation energy source particularly for fuel cells and modern industries, but serious limitations because of its lower explosive level (LEL) (4% in normal air) demands the development of high performance sensing devices. Among the several types, metal oxide based semiconductor gas sensors tin oxide is the most widely investigated. Tin oxide exists as SnO_2 and SnO, with the oxidation states of +4 and +2 respectively. SnO_2 is a wide band gap n-type semiconductor due to the intrinsic oxygen vacancies whereas SnO shows high p-type conductivity due to the naturally formed Sn vacancies. Even though SnO_2, the most stable of the phases has been widely studied, SnO has not been investigated to a large extent primarily because of its ease of transformation into SnO_2. Nevertheless the p-type character of SnO along with the possibility of formation of heterojunction (in the mixed phase SnO/SnO_2 system) makes it a suitable alternative material that needs to be studied for gas sensing applications. Formation of p-n junctions to improve the sensing performance has been proved in CuO/SnO_2, NiO/SnO_2 etc. systems however the combination of SnO/SnO_2 for sensing applications has not been explored.

Here we present the synthesis of of SnO/SnO_2 and SnO_x ($1<x<2$) microcubes via a simple hydrothermal synthesis route, and demonstrate their efficient H_2 sensing capability. To highlight the improved performance of this system the gas sensing studies were performed on pure SnO_2. The stretching of the lower limit of detection and the room temperature response was achieved by the incorporation of palladium into the SnO/SnO_2 material. Selectivity was established by observing the response in the presence of interfering gases like, EtOH, Acetone and NH_3.

2. Synthesis Procedures

Tin (II) acetate ($C_4H_6O_4Sn$), palladium (II) chloride ($PdCl_2$), poly ethylene glycol (PEG-400), NaOH and Ethanol used for synthesis by hydrothermal conditions. Different weight percentages of palladium were incorporated by the impregnation method using palladium chloride ($PdCl_2$). Sodium Borohydride was used to reduce palladium salt to metallic palladium.

Fabrication of Sensor device and the schematic of the sensor assembly with the sensor characteristics measurement setup are described elsewhere [1]

3. Results and Discussion

3.1. Powder X-Ray Diffraction

The chemical composition and crystal structure of the as synthesized sample were confirmed by powder X-Ray diffraction. XRD of the synthesised material shows (Fig.1.) well resolved diffraction peaks in the range of 2θ = 10 - 65° are perfectly indexed to the rutile SnO_2 and tetragonal structure of SnO. The calculated lattice constants for SnO (a=3.796 A°, C=4.816 A°) and SnO_2 (a= 4.740 A°, C=3.190 A°), are consistent with the standard reported values.

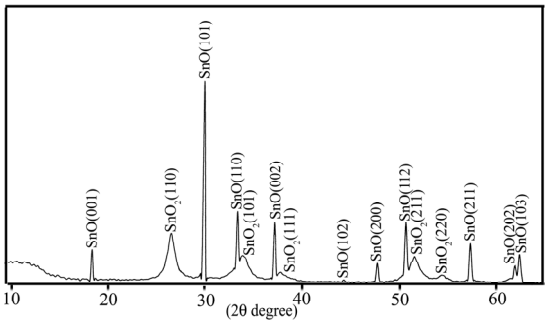

Fig.1. Powder X-Ray diffraction pattern of the as synthesized sample.

3.2. Micro-Raman Spectroscopy

Raman spectroscopy is one of the powerful methods to analyze crystal structure and crystal phase. Fig.2 shows the room temperature Raman spectra of the as synthesized materials, with the three SnO_2 Raman active modes one SnO active mode and two transition metal oxide phases.

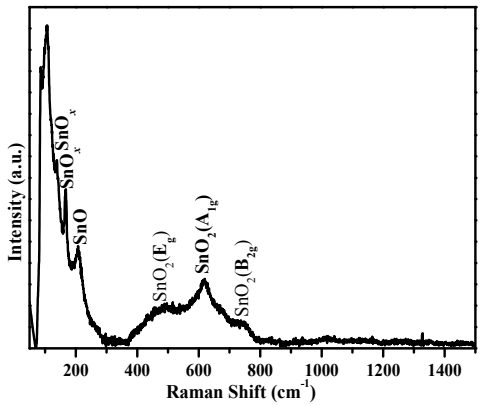

Fig.2. Raman spectra of as synthesized Sample.

The Raman shifts at 493, 626, 751cm^{-1} can assigned to the fundamental Raman active modes of SnO_2, the peak at 626 cm^{-1} attributed to the Sn-O stretching vibrational mode (A1g) [2]. The peaks at 470 and 750 cm^{-1} correspond to the fundamental vibrational modes of Eg and B2g respectively. [3] Whereas the peak position at 208 cm^{-1} assigned to the SnO active mode [4]. The peak positioned at 136 and 170 cm^{-1} may attributed to the transition oxide (SnO_x) where $1 < x < 2$. [4]. we also observed that, the Raman active modes were slightly shifted (~5 cm^{-1}) towards the lower frequency region, presumably due to lattice defects.

The FTIR studies show the characteristic band at 627 cm^{-1} assigned to the Sn-O-Sn vibration which is also the Raman active mode. The shoulder observed at 560 cm^{-1} is assign to Sn-O vibrations.

The thermal behaviour of the as synthesised materials was studied by Thermo-Gravimetric and Differential Thermal analysis from RT to 700°C at the rate of 10°C/ min. The thermo gram shows two exothermic peaks associated with the phase transition. Mass loss was observed upto 400° C due to the removal of water/OH groups and PEG respectively. The sharp weight loss occurs from 400 to 600° C due to the rearrangement of crystal structure and phase changes, form 600 to 700° C the sample mass increased upto 2%, most probably due to the addition of oxygen. This indicates that the SnO is not thermally stable, and it is converted to SnO_2 at higher temperatures. This is also conformed through XRD (not shown).Total weight loss during the thermal studies is about 4%.

The typical magnetic hysteresis curve shows in the Fig.3 To confirm the presence of oxygen vacancies magnetization studies were carried out. The binary and ternary oxides of tin such as SnO_2, Sn_3O_4, SnO are known to non-ferromagnetic in nature.

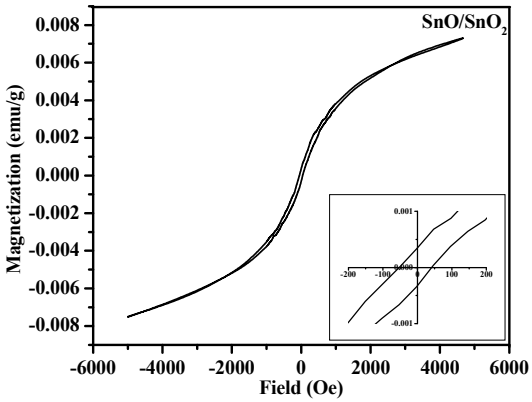

Fig.3. Magnetization hysteresis loop of SnO/SnO_2 structures at room temperature. The inset shows the magnified curves near H = 0

The magnetization (M) versus field (H) exhibits the ferromagnetic behavior at room temperature with the saturation magnetization 0.008 (emu/g). Origin of the ferromagnetic behavior could be attributed to oxygen vacancies in the as synthesized materials.

3.3. X-ray photo electron Spectroscopy

We also carried out the X-ray photoelectron spectroscopy (XPS) studies to know the surface composition, chemical states, and binding energy of the as synthesized samples. The energy scale of the spectrometer has been calibrated with binding energy of C1s taken at 284.6 eV. Except for peaks corresponding to Sn, O, and C no other impurities were detected.

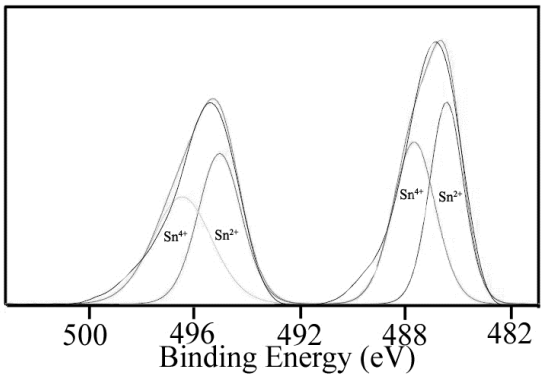

Fig. 4. Core level XPS spectra of Sn 3d peak

The Fig.4 shows that the Sn 3d spectrum of the as prepared sample which could be assigned to the spin orbit doublelet for Sn^{4+} at 487.6 eV ($3d_{5/2}$) and 496.1eV ($3d_{3/2}$) the Sn^{2+} peak positioned at 486.3 eV ($3d_{5/2}$) 494.6 eV ($3d_{3/2}$). The spin orbit splitting energy of 8.4 eV is in agreement with literature values [5, 6].

3.4. Structure and Morphology evaluation of the synthesized products

The formation of SnO/SnO_2 micro cubes was followed by observing the samples during various stages of the synthesis procedure. The SEM images present the morphological evolution where Fig.5(a) shows the as synthesized nanorods followed by aggregation of nanorods to form micro cubes as is evident from the intermediate step Fig.5(b). After completion of the reaction micro cubes formed are shown in Fig.5(c).

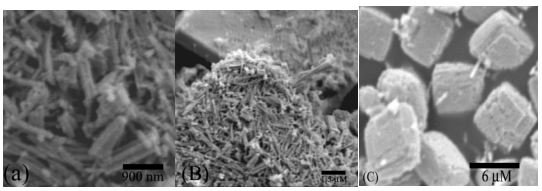

Fig.5. Series of SEM images revealing the morphology evolution

3.5. Gas sensing studies

The gas sensing measurements were carried out by measuring the resistance change, caused by adsorption and desorption of gas molecules on the surface of the sensing materials. The sensitivity is defined as ratio of change of sensor resistance in the presence of gas (R_{air}-R_{gas}) normalised to the resistance in the presence of air (R_{air}). The sensing responses of pure SnO_2, SnO/SnO_2, $SnO/SnO_2/Pd_{0.1\%}$ and $SnO/SnO2/Pd_{0.2\%}$ to 10% hydrogen gas as function operating temperatures are given in the Fig. 6 and 7.

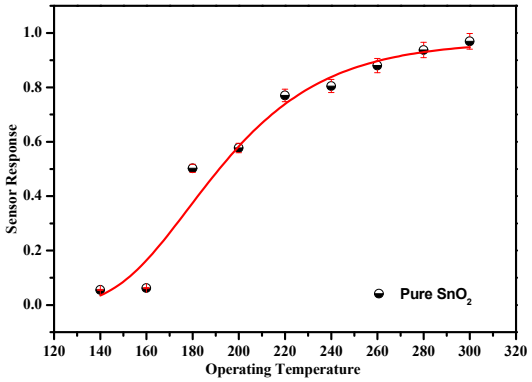

Fig.6. Sensor response versus temperature for pure SnO_2 for 10% Hydrogen gas.

Pure SnO_2 (Fig.6) had the highest sensitivity around ~260°C, in contrast the synthesized SnO/SnO_2 mixtures (Fig.7) reaches the maximum response around 120°C. In order to improve the sensitivity, reduce the operating temperature and make the sensing device highly selective different wt. percentages of palladium was incorporated. The SEM-EDX analysis was used to confirm the % of Pd incorporated in the synthesized materials.

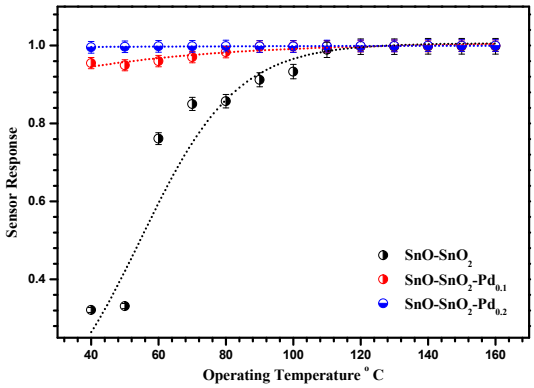

Fig.7.Sensor response of SnO/SnO_2, $SnO/SnO_2/Pd_{(0.1\%)}$, $SnO\text{-}SnO_2\text{-}Pd_{(0.2\%)}$ towards 10% Hydrogen gas at different operating temperature.

The effect of palladium loading level towards hydrogen sensing was examined to determine optimal loading. A loading of $0.1_{wt\%}$ Pd shows the maximum sensitivity at on operating temperature of 70° C, whereas loading of $0.2_{wt\%}$ Pd shows the maximum response at room temperature.

By varying the gas concentrations, we further carried out the gas sensing measurements to

obtain the response characteristics. The hydrogen gas was diluted from 100% to 0.25% by nitrogen gas. Fig.8 shows the response of $SnO/SnO_2/Pd_{(0.2wt\%)}$ to different concentrations of hydrogen at different operating temperatures from 50 to 100° C. The sensor shows the maximum response even at room temperature for 0.25% hydrogen in nitrogen. It is noteworthy that the sensor could sense hydrogen even less than 500 ppm at room temperature.

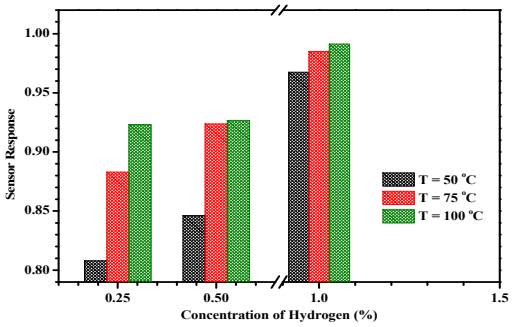

Fig.8. Sensor response of $SnO/SnO_2/Pd(0.2wt\%)$ versus concentration of Hydrogen in air at different temperatures.

As expected the sensor response shows follows the sigmoidal curve with increasing concentration of hydrogen. The selectivity (Fig.9) was established by testing the sensing device to other interfering gases like ethanol, acetone, and ammonia, (taken as 10% concentration in air) at different operating temperatures. At room temperatures the changes of sensor resistance for interfering is less than 1 order.

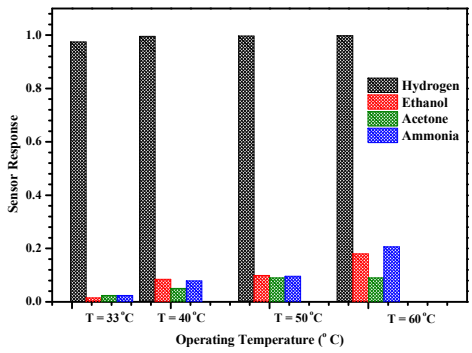

Fig.9. Sensor response of $SnO/SnO_2/Pd_{(0.2wt\%)}$ at different operating temperatures

3.6. Sensing Mechanisms

The enhancement of gas sensing response in SnO/SnO_2 mixtures can be postulated on the following lines. SnO_2 is a well known n-type semiconducting oxide capable of recognizing any reducing test gases by an increase in its electrical conductivity (σ). In the SnO/SnO_2 at the heterojunction formed at the interface of n-SnO_2 and p-SnO in the presence of the reducing gas the band bending is further enhanced leading to tunneling across the junction and increased mobility (μ) contributing to increase in conductivity.

The multiple role of Pd in the gas sensing can be explained as follows. Pd assists the adsorption of H_2 on the sensor surface because of its affinity and ionizes the gas releasing electrons into the conduction band. In addition as has been reported earlier Pd also helps in modulating the surface work-function contributing the increased the sensor response [7]

3.7. Conclusions

In summary, SnO/SnO_2 mixtures were synthesized by the simple hydrothermal method. Gas sensing properties of the as synthesized materials showed an enhanced sensing response compared to pure SnO_2. The SnO/SnO_2 heterojunctions showed excellent hydrogen sensing response. Incorporation of 0.2%Pd imparted it highly selective room temperature sensing capability. Our studies have revealed the role of p-n junctions and palladium incorporation in achieving this excellent sensor response.

References

[1] S.V. Manorama, G. Sarala Devi, V.J. Rao, Hydrogen sulfide sensor based on tinoxide deposited by spray pyrolysis and microwave plasma chemical apordeposition, *Appl. Phys. Lett.* 64 (1994) 3163–3165. doi.org/10.1063/1.111326

[2] A. Yu, R. Frech, Mesoporous tin oxides as lithium intercalation anode materials, *J. Power Sources* 104 (2002) 97–100

[3] J.S. Lee, S.K. Sim, B.Min, K. Cho, S.W. Kim, S. Kim, Structural and optoelectronicproperties of SnO2 nanowires synthesized from ball-milled SnO2 powders, *J.Cryst. Growth* 267 (2004) 145–149.

[4] James L. Gole, Alexei V. Iretskii, Mark G. White, Amanda Jacob,W. Brent Carter, Sharka M. Prokes,| and Ann S. EricksonSuggested Oxidation State Dependence for the Activity of Submicron Structures Prepared from Tin/Tin Oxide Mixtures *Chem. Mater.* 2004, 16, 5473-5481

[5] Fang Song, Huilan Su, Jianjun Chen, Won-Jin Moon, Woon Ming Laucd and Di Zhang 3D hierarchical porous SnO_2 derived from self-assembled biological systems for superior gas sensing application *Journal of Materials Chemistry* DOI: 10.1039/c1jm1344

[6] Andrei Kolmakov, Sai Potluri, Alexei Barinov, Tevfik O. Mentes, Luca Gregoratti, Miguel A. Nin o, Andrea Locatelli,and Maya Kisk inova Spectromicroscopy for Addressing the Surface and Electron TransportProperties of Individual 1-D Nanostructures and Their Networks *ACS Nano* VOL. 2 ▪ NO. 10 ▪ 1993–2000 ▪ 2008

[7] C. V. Gopal Reddy and S. V. Manorama Room Temperature Hydrogen Sensor Based on SnO_2:La_2O_3 *Journal of The Electrochemical Society*, 147 (1) 390-393 (2000).